

Published in final edited form as:

Chem Biol Interact. 2012 March 5; 196(1-2): 1–10. doi:10.1016/j.cbi.2012.01.004.

The Naphthol Selective Estrogen Receptor Modulator (SERM), LY2066948, is Oxidized to an *o*-Quinone Analogous to the Naphthol Equine Estrogen, Equilenin

Teshome B. Gherezghiher, Bradley Michalsen, R. Esala P. Chandrasena, Zhihui Qin, Johann Sohn, Gregory R.J. Thatcher, and Judy L. Bolton*

Department of Medicinal Chemistry and Pharmacognosy College of Pharmacy University of Illinois at Chicago 833 S. Wood Street, M/C 781, Chicago, IL 60612-7231, USA

Abstract

o-Quinone forming estrogens and selective estrogen receptor modulators (SERMs) have been associated with carcinogenesis. LY2066948, a novel SERM in development by Eli Lilly for the treatment of uterine fibroids and myomas, has structural similarity to the equine estrogen equilenin present in hormone replacement formulations; both contain a naphthol group susceptible to oxidative metabolism to *o*-quinones. LY2066948 was synthesized and assayed for antiestrogenic activity, and in cell culture was confirmed to be a more potent antiestrogen than the prototypical SERM, 4-hydroxytamoxifen. Oxidation of LY2066948 with 2-iodoxybenzoic acid gave an *o*-quinone ($t_{1/2} = 3.9 \pm 0.1$ h) which like 4-hydroxyequilenin-*o*-quinone ($t_{1/2} = 2.5 \pm 0.2$ h) was observed to be exceptionally long-lived with the potential to cause cytotoxicity and/or genotoxicity. In model reactions with tyrosinase, the catechol metabolites of LY2066948 and equilenin were products; interestingly, in the presence of ascorbate to inhibit autoxidation, these catechols were formed quantitatively. Tyrosinase incubations in the presence of GSH gave the expected GSH conjugates resulting from trapping of the *o*-quinones, which were characterized by LC-MS/MS. Incubations of LY2066948 or equilenin with rat liver microsomes also gave detectable *o*-quinone trapped GSH conjugates; however, as observed with other SERMs, oxidative metabolism of LY2066948 mainly occurred on the amino side chain to yield the *N*-dealkylated metabolite. CYP1B1 is believed to be responsible for extra-hepatic generation of genotoxic estrogen quinones and *o*-quinone GSH conjugates were detected in equilenin incubations. However, in corresponding incubations with CYP1B1 supersomes, *noo*-quinone GSH conjugates of LY2066948 were detected. These studies suggest that although the naphthol group is susceptible to oxidative metabolism to long-lived *o*-quinones, the formation of these quinones by cytochrome P450 can be attenuated by the chemistry of the remainder of the molecule as in the case of LY2066948.

Keywords

estrogen; equilenin; LY2066948; cytochrome P450; *o*-quinone; SERM

© 2012 Elsevier Ireland Ltd. All rights reserved

*To whom correspondence should be addressed. Tel: (312) 996-5280, FAX: (312) 996-7170, Judy.Bolton@uic.edu.

Publisher's Disclaimer: This is a PDF file of an unedited manuscript that has been accepted for publication. As a service to our customers we are providing this early version of the manuscript. The manuscript will undergo copyediting, typesetting, and review of the resulting proof before it is published in its final citable form. Please note that during the production process errors may be discovered which could affect the content, and all legal disclaimers that apply to the journal pertain.

1. Introduction

Selective estrogen receptor modulators (SERMs) are compounds that display estrogen receptor (ER) agonist or antagonist activity depending on the target tissue [1, 2]. Currently, four SERMs are approved by the FDA for clinical use: tamoxifen for prevention and treatment of ER-positive breast cancer, toremifene for the treatment of ER-positive breast cancer, clomifene for infertility treatment, and raloxifene both for the treatment and prevention of osteoporosis in postmenopausal women, and also for the reduction in risk of invasive breast cancer in postmenopausal women at high risk [2, 3]. Unfortunately, all of these SERMs have side effects making the development of an ideal SERM significant for postmenopausal women [3, 4]. The perfect SERM would act as an agonist in bone to prevent osteoporosis, in the heart to prevent cardiovascular disease, and in the CNS to prevent hot flashes and neurological disorders such as Alzheimer's disease [5]. Conversely, the perfect SERM would act as an antagonist in hormone sensitive tissues to prevent breast cancer without increasing the risk of endometrial cancer and venous thromboembolism. In search of an ideal SERM, a new-generation of SERMs such as lasofoxifene and bazedoxifene are currently in clinical trials and LY2066948 (Scheme 1) is in clinical development by Eli Lilly for the potential treatment of uterine fibroids and myomas [3, 6–8].

Although tamoxifen is effective in treating and preventing ER positive breast cancer [3], it increases the incidence of endometrial cancer [9–11]. This disturbing side effect shows the importance of fully understanding the bioactivation pathways and mechanisms of toxicity of tamoxifen and related SERMs, since they are in widespread use as preventive drugs in high risk but otherwise healthy individuals [1]. In addition, to the widely accepted hormonal mechanism of SERM carcinogenesis, another potential carcinogenic mechanism could involve the bioactivation of SERMs by cytochrome P450 to form redox active and/or electrophilic metabolites, which act as chemical carcinogens by modifying cellular macromolecules [12, 13]. For example, four different types of electrophilic metabolites have been reported for SERMs [1]. The most genotoxic metabolite is likely the highly reactive carbocation formed from tamoxifen, which has been implicated in DNA alkylation [14–16]. The second bioactivation pathway involves oxidation of tamoxifen, or the benzopyran SERM acolbifene, to classical quinonemethides [17, 18]. Di-quinonemethides have been generated during oxidation of raloxifene [19], desmethylarloxifene (DMA) [20], and acolbifene [18]. The fourth bioactivation pathway for SERMs involves *o*-quinone formation which has been implicated in tamoxifen protein binding [21, 22] and is the major cytotoxic pathway for endogenous and equine estrogens (Scheme 1) [22–24].

LY2066948, a new SERM which is under development by Eli Lilly, binds with high affinity to estrogen receptors ER α and ER β and shows potent antiestrogenic activity as measured by inhibition of estradiol-mediated induction of alkaline phosphatase activity in Ishikawa endometrial cancer cells [6, 25]. Similar to the equine estrogen equilenin (EN, Scheme 1), which is present in the hormone replacement formulations, Prempro® and Premarin®, LY2066948 contains a naphthol structure (Scheme 1). The presence of an unsaturated B ring (Scheme 1) in EN generally leads to exclusive 4-hydroxylation by enzymatic oxidation, which in turn results in the formation of a highly reactive *o*-quinone [1, 23] causing oxidation and alkylation of DNA *in vitro* and *in vivo* [21, 26–28]. In the current study, we hypothesized that since 4-OHEN-*o*-quinone is the major phase I metabolite of EN, it is likely that LY2066948 is also oxidized to a 3,4-*o*-quinone which could display similar cytotoxic potential.

2. Materials and Methods

2.1. Caution

LY2066948-o-quinone was handled in accordance with the NIH Guidelines for the Laboratory Use of Chemical Carcinogens [29].

2.2. Materials

All solvents and chemicals were purchased from Aldrich Chemical (Milwaukee, WI), Fisher Scientific (Itasca, IL), or Sigma (St. Louis, MO) unless stated otherwise. EN was purchased from Steraloids Inc. (Newport, RI). Human P450 supersomes were obtained from BD Biosciences (Woburn, MA).

2.3. Instrumentation

NMR spectra were recorded on either a BrukerAvance 400 MHz spectrometer or Bruker DPX 400 MHz spectrometer. UV spectra were obtained on a Hewlett-Packard (Palo Alto, CA) 8452A photodiode array UV/Vis spectrometer. HPLC analysis was performed using an Agilent (Palo Alto, CA) 1100 instrument measuring UV absorbance at 280 nm. LC-MS/MS was carried out using an Agilent 6310 ion trap mass spectrometer (Agilent Technologies, Santa Clara, CA) equipped with an electrospray ionization source. Ions were detected in positive ion mode using CID ionization with a resolving power of 5,000 FWHM and mass accuracy of 0.1 amu.

2.4. HPLC Methodology

Two general methods were used to analyze metabolites and GSH conjugates. In method A, an Agilent Eclipse XDB-C18 column (4.6 mm × 150 mm, 5 μm) was used for LC-MS analysis of tyrosinase and rat liver microsomal incubations. The mobile phase consisted of solvent A, water containing 10% methanol (v/v) and 0.1% formic acid (v/v) and solvent B, acetonitrile and 0.1% formic acid (v/v). For LY2066948 analysis, the mobile phase consisted of a linear gradient from 5 to 30% acetonitrile (v/v) over 20 min, 10 min gradient from 30 to 60% acetonitrile (v/v), and then 60 to 90% acetonitrile (v/v) over 5 min. In method B, a Beckman (4.6 mm × 150 mm, 5 μm) Ultrasphere C18 column was used. The mobile phase consisted of a linear gradient from 10 to 30% acetonitrile (v/v) in water over 15 min, 10 min gradient from 30 to 60% acetonitrile (v/v), and then 60 – 90% acetonitrile (v/v) over 5 min. A flow rate of 1.0 mL/min was used for all analyses. All reported retention times were obtained using method A unless stated otherwise.

2.5. Synthesis of LY2066948

LY2066948 was synthesized according to the method reported by Hummel et al. [25] with minor modification. Specifically, yield of intermediate **4** (Scheme 2) was increased from 30% (Hummel method) to 50% through the addition of cesium carbonate along with a stoichiometric amount of 1-naphthoic acid during coupling of intermediates **2** and **3** (Scheme 2) [30]. LY2066948: ¹H NMR (400 MHz, CDCl₃): δ 1.49 (m, 2H), 1.69 (m, 4H), 2.61 (m, 4H), 2.81 (t, *J* = 5.6 Hz, 2H), 3.06 (s, 3H), 3.99 (t, *J* = 5.6 Hz, 2H), 6.42 (s, 4H), 7.02 (dd, *J* = 9.2, 2.4 Hz, 1H), 7.12 (d, *J* = 2.0 Hz, 1H), 7.41 (d, *J* = 8.8 Hz, 1H), 7.58 (d, *J* = 8.8 Hz, 1H), 7.69 (d, *J* = 8.4 Hz, 2H), 7.79 (d, *J* = 9.2 Hz, 1H), 7.88 (d, *J* = 8.4, 2H). UV (CH₃OH): 226, 270 nm; positive ion electrospray mass spectroscopy *m/z* 518.19 (100%) [M + H]⁺.

2.6. Cell Culture

The MCF-7 cell line (MCF-7 WS8) was provided by V. C. Jordan (Fox Chase Cancer Center, Philadelphia, PA) and was originally acquired from the Michigan Cancer

Foundation (Detroit, MI). This estrogen receptor positive breast cancer cell line is used as a model for hormone responsive breast cancer, and thus far no significant differences have been observed between the parental MCF-7 cell line and the MCF-7 WS8 cells [31, 32]. Previously, the growth behavior and estrogen responsiveness was characterized in detail [33]. The Ishikawa/ECC-1 cell line was provided by Dr. R. B. Hochberg (Yale University, New Haven, CT). Ishikawa/ECC-1 is a well-differentiated human endometrial cancer cell line which displays estrogen-inducible alkaline phosphatase activity [34–36]. To authenticate this cell line, the short tandem repeat profile (STR) was determined using the StemElite kit by Promega according to the manufacturer's instructions. The PCR products were analyzed with the 3730 XL ABI genetic analyzer. The STR profile of this cell line was in accordance with the STR profile of Ishikawa according to the Health Protection Agency Culture collection in the UK and with the STR profile of ECC-1 cells according to the ATTC database.

MCF-7 WS8 cells were cultured in RPMI 1640 media containing 1% glutamax-1, 1% NEAA, 0.05% insulin, and 5% heat-inactivated fetal bovine serum (FBS). Ishikawa/ECC-1 cells were grown in Dulbecco's Modified Eagle medium (DMEM/F12) containing 1% sodium pyruvate, 1% non-essential amino acids (NEAA), 1% glutamax-1, 0.05% insulin, and 10% heat-inactivated FBS. All cultures were maintained at 37 °C inside humidified incubator with 5% CO₂:95% air. For phenol-free complete medium, stripped FBS was used. Stripped serum was prepared by incubating the serum with acetone-washed activated charcoal (100 mg/mL) at 4 °C for 30 min, and centrifuged at 4000g at 4 °C for 15 min. The whole procedure for preparing stripped FBS was repeated three times.

2.6.1. Alkaline Phosphatase Induction in Ishikawa/ECC-1 Cells—Alkaline phosphatase activity in Ishikawa/ECC-1 cells was measured using the protocol as described previously [35, 37]. Cells (1.5×10^4 cells/190 L/well) were preincubated in 96-well plates overnight in estrogen-free medium. Test samples (10 L at varying concentrations in DMSO) were added to determine EC₅₀ values, and the cells in a total volume of 200 L media/well were incubated at 37°C for 4 days. For the determination of antiestrogenic activity, 2×10^{-8} M E₂ was added to the media. After removing the culture medium, the induction plates were washed with PBS, and 0.01% Triton $\times 100$ in 0.1 M Tris buffer (50 L, pH 9.8) was added. An aliquot (150 L) of 24 mM *p*-nitrophenyl phosphate (phosphatase substrate) was added to each well. The enzyme activity was measured by reading the release of *p*-nitrophenol at 405 nm every 15 s with a 10 s shake between readings for 16 readings using a Power Wave 200 microplate scanning spectrophotometer (Bio-Tek Instruments, Winooski, VT). The maximal slopes of the lines generated by the kinetic readings representing the rate of formation of *p*-nitrophenol were calculated. For antiestrogenic determination, the percent induction as compared with the background induction control was calculated using the following equation: $[1 - ((\text{slope}_{\text{sample}} - \text{slope}_{\text{cells}}) / (\text{slope}_{\text{estrogen}} - \text{slope}_{\text{cells}}))] \times 100 = \% \text{ antiestrogenic induction}$. All experiments were run in triplicate.

2.6.2. ERE-Luciferase Assay—After MCF-7 WS8 cells were grown for 72 h in phenol-free medium, cells were trypsinized and resuspended at 1×10^7 cells/mL of serum-free medium. Incubation of cells (5×10^6) with 3 μ g pERE-luciferase plasmid (V. C. Jordan) and 1 μ g pRL-TK plasmid (Promega, Madison, WI) were done in a 4 mm gap cuvette for 5 min at room temperature before electroporation at 950 μ F and 250 V using the GenePulserXcell (BioRad Laboratories, Hercules, CA). Transfected cells were diluted in serum containing medium and plated in 6-well plates (8.0×10^5 cells/well). Following a 24 h recovery period, the cells were washed with PBS and treated with either compound or control for an additional 24 h. To check ERE-luciferase activity, the Dual-Luciferase Reporter Assay System (Promega) was used. Cell lysates (20 μ L) from treated MCF-7 WS8 cells were placed in 96 well plates. Luciferase Assay Reagent II (100 μ L) was added followed by a 12 s

read by a FLUOstar OPTIMA (BMG Lab Tech, Offenburg, Germany). Stop &Glo® (100 µL) was added followed by a 12 s read, thus allowing for termination of firefly luciferase activity and activation of renilla activity. The sample results were normalized to pRL-TK, to account for transfection efficiency, by dividing the sum of the luciferase activity by the sum of the renilla activity. All experiments were run in triplicate, and data was analyzed using one way ANOVA.

2.7. Kinetic Studies of LY2066948-*o*-Quinone or 4-OHEN-*o*-Quinone

A mixture of LY2066948 (0.6 mM) in anhydrous methanol (200 µL) and 2-iodoxybenzoic acid (IBX, 18 mM) was stirred for 1 min at room temperature. A yellow color developed in 30 s and the mixture was filtered and analyzed immediately. An aliquot (0.1 mL) of LY2066948-*o*-quinone (60 µM) was then added to 50 mM phosphate buffer (0.9 mL, pH 7.4) at 37 °C. An identical procedure was used to prepare 4-OHEN-*o*-quinone. The disappearance of the *o*-quinones were monitored by measuring the decrease in UV absorbance at 378 nm (LY2066948-*o*-quinone) and 392 nm (4-OHEN-*o*-quinone) using a Hewlett-Packard 8452A diode array spectrometer. The half-life for each *o*-quinone was determined by measuring the respective pseudo-first-order rates of decay according to the equation $t_{1/2} = \ln(2)/k$.

2.8. Incubations with Tyrosinase

Solutions containing substrate (30 µM), tyrosinase (0.1 mg/mL), and GSH (1 mM) in 50 mM phosphate buffer (pH 7.4, 0.5 mL total volume) were incubated at 37 °C for 30 min. The incubations were quenched by chilling in ice followed by addition of perchloric acid (25 µL). Control incubations were carried out without tyrosinase or GSH. Incubation mixtures were centrifuged at 10640g at 4 °C for 10 min. Supernatants were filtered and analyzed by LC-MS/MS and HPLC method A. The above incubations were repeated in the presence of ascorbic acid (1 mM) solution without GSH.

2.9. Incubations with Liver Microsomes

Female Sprague-Dawley rats (200 – 220 g) were obtained from Sasco Inc. (Omaha, NE). To induce CYP3A isozymes, rats were pretreated with 100 mg/kg dexamethasone (i.p. in corn oil) daily for 3 consecutive days and were sacrificed on day 4. Rat liver microsomes were prepared and protein and P450 concentrations were determined as described previously [38]. Solutions containing substrate (30 µM), rat liver microsomes (1 nmol P450/mL), NADPH (1 mM), GSH (1 mM) in 50 mM phosphate buffer (pH 7.4, 0.5 mL total volume) were incubated at 37 °C for 30 min. For control incubations, either NADPH or GSH was omitted. The reactions were quenched by chilling in ice followed by addition of perchloric acid (25 µL). Proteins were removed by centrifugation at 10640g for 10 min. Supernatants were filtered and analyzed by LC-MS/MS and HPLC method B. Similar methodology was employed in incubations with human liver microsomes (pooled from 15 individuals, In Vitro Technologies, Baltimore, MD) except the concentration of P450 used was 0.34 nmol/mL.

2.10. Incubations with CYP3A4 and CYP1B1 Supersomes

Solutions containing substrate (30 µM), CYP3A4 or CYP1B1 (10 pmol/mL), NADPH (1 mM), GSH (1 mM) in 50 mM phosphate buffer (pH 7.4, 0.5 mL total volume) was incubated at 37 °C for 30 min. For control incubations, either NADPH or GSH was omitted. Reactions were quenched by chilling in ice followed by addition of perchloric acid (25 µL). Proteins were removed by centrifugation at 10640g for 10 min. Supernatants were filtered and analyzed by LC-MS/MS and HPLC using method A.

3. Results

3.1. Antiestrogenic Activity of LY2066948

Alkaline phosphatase activity in the Ishikawa/ECC-1 cell line was measured as the end point for relative estrogenic stimulation in both agonist and antagonist modes (dose response for the SERMs to block the stimulatory effect of a fixed dose of E₂) [6, 25]. In antagonist mode, LY2066948 blocked the estrogenic effects of E₂ (0.9 nM) with an IC₅₀ of 1.8 ± 0.50 nM, compared with an IC₅₀ of 9.0 ± 1.9 nM for 4-hydroxytamoxifen (Figure 1A). These data are consistent with previous studies reported by Geiser et al.[6], which showed that LY2066948 was a more potent antagonist of estradiol-induced uterine cell proliferation than 4-hydroxytamoxifen.

We also confirmed the antiestrogenic activity of LY2066948 using the ERE-luciferase assay in MCF-7 WS8 cells transiently transfected with the pERE-luciferase construct [39]. Inhibition of estradiol-induced luciferase induction in this cell line reflects the ability of antiestrogenic compounds to inhibit estrogen regulated transcription and luciferase reporter expression. At concentrations of 5 nM and 10 nM 4-hydroxytamoxifen, luciferase induction in the presence of 1 nM estradiol was observed to be 83 ± 3.0% and 46 ± 9.7%, respectively (1 nM estradiol = 100%). By comparison, similar concentrations of LY2066948 gave respective inductions of 54 ± 0.7% and 24 ± 1.0% (Figure 1B). These data are consistent with earlier studies which demonstrate LY2066948 as a potent antiestrogen in mammary tissue [6]. All data represent the average ± SD for triplicate determinations of duplicate experiments.

3.2. Kinetic Studies of LY2066948-*o*-Quinone or 4-OHEN-*o*-Quinone

The LY2066948-*o*-quinone was generated by IBX oxidation and the reactivity of the *o*-quinone was examined (Figure 2A). Absent from the spectrum of LY2066948 itself, a strong absorbance at 378 nm was observed in the UV spectrum of the LY2066948-*o*-quinone (Figure 2A), which was similar to the UV spectrum of the 4-OHEN-*o*-quinone [$\lambda_{\text{max}} = 392$ nm, Figure 2B, [22]]. A protonated molecular ion at m/z 532 [M+H]⁺ (data not shown) was also observed in the positive ion electrospray mass spectrum of LY2066948-*o*-quinone, corresponding to two mass units less than that of catechol LY2066948. The rate of disappearance of LY2066948-*o*-quinone was determined and the half-life at physiological pH and temperature was approximately 3.9 ± 0.1 h (Figure 2A). For comparison, 4-OHEN-*o*-quinone was also prepared from EN using IBX as an oxidizing agent and its rate of disappearance was determined under the same conditions. The half-life was approximately 2.5 ± 0.2 h (Figure 2B) which is consistent with the previously reported value of 2.3 h [22], within experimental error.

3.3. Incubation of LY2066948 or Equilenin with Tyrosinase

The oxidative metabolism of LY2066948 was investigated under various oxidative conditions as summarized in Scheme 3. Incubations with tyrosinase in the presence of GSH produced mono-GSH and di-GSH conjugates (Figure 3A) resulting from trapping of the *o*-quinones. We identified the mono-GSH conjugate based on the detection of a strong [M + H]⁺ peak at m/z 837 as well as its tandem MS spectrum (Figure 4A). The base peak at m/z 744 came from the loss of water and the glycine residue, and the product ions at m/z 819 and m/z 708 were formed by elimination of water and loss of the γ -glutamyl group, respectively. The product ion at m/z 564 was generated by cleavage adjacent to the thioether moiety with charge retention on the LY2066948 residue (Figure 4A). These types of fragmentations are characteristic of GSH conjugates [40]. The LY2066948 di-GSH conjugate was also observed as a doubly charged ion at m/z 571 [M + 2H]²⁺ (data not shown). Similarly, when equilenin was incubated with tyrosinase in the presence of GSH, mono and di-GSH conjugates were detected (Figure 3B) with identical mass spectra as reported previously

[41]. Incubation of LY2066948 with tyrosinase in the presence ascorbate as a reducing agent quantitatively converted LY2066948 to its catechol (Figure 3A). Similarly, when equilenin was incubated with tyrosinase and ascorbate, 4-OHEN was the major product (Figure 3B).

3.4. Incubation of LY2066948 or Equilenin with Liver Microsomes

In the presence of rat liver microsomes, NADPH, and GSH, LY2066948 was oxidized to an *o*-quinone, which was trapped by GSH to produce one di-GSH conjugate (Figure 5A). This conjugate was identified based on the detection of $[M + 2H]^{2+}$ peak at m/z 571 (data not shown). In addition to the di-GSH conjugate, the *N*-dealkylated primary amine metabolite (Figure 5A) was formed as a major product, and was identified based on the detection of $[M + H]^+$ peak at m/z 450 (Figure 4B). MS/MS analysis of the molecular ion at m/z 450 produced fragment ions at m/z 406, 371, 314, and 234, corresponding to the loss of ethylamine moiety, cleavage of methyl sulfonyl moiety, loss of 2-phenoxyethylamine, and the concurrent loss of methyl sulfonyl and 2-phenoxyethylamine moieties, respectively (Figure 4B). In contrast, no GSH conjugates were obtained in the incubation of LY2066948 with human liver microsomes (data not shown). For comparison, we also reinvestigated the metabolism of equilenin by rat liver microsomes in the presence of NADPH and GSH. Mono and di-GSH conjugates were detected as in the tyrosinase incubations described above resulting from trapping of 4-OHEN-*o*-quinone with GSH (Figure 5B). In addition, 17 β -equilenin was formed in rat liver microsomal incubations and further oxidized to *o*-quinone to give a di-GSH conjugate as a metabolite (Figure 5B). Identification of 17 β -equilenin and its corresponding di-GSH conjugate was based on detection of the corresponding molecular ions at m/z 267 and 893, respectively, and also by comparison of retention times and tandem mass spectra to authentic standards.

3.5. Incubation of LY2066948 or Equilenin with CYP3A4 and CYP1B1 Supersomes

It is known that human CYP3A4 contributes to the metabolism of about half the drugs in use today [42]. Incubation of LY2066948 with CYP3A4 supersomes also gave the LY2066948-*o*-quinone di-GSH conjugate as a minor metabolite (4%) and the *N*-dealkylated primary amine metabolite (17%) as the major product (Figure 5A). In contrast, no GSH conjugates were observed when equilenin was incubated with CYP3A4 in the presence of NADPH and GSH (Figure 5B). Similarly, in experiments with CYP1B1 supersomes, the major extra-hepatic isozyme responsible for catechol estrogen formation [43], no LY2066948-*o*-quinone GSH conjugates were detected (Figure 6A). However, CYP1B1 appears to be effective at oxidizing equilenin to *o*-quinone as is indicated by detection of GSH conjugates. In addition to these GSH conjugates, 17 β -equilenin was detected as a major metabolite of equilenin and formation of this metabolite was not NADPH dependent (Figure 6B). Reduction of the 17-ketone moiety by several human CYP isoforms has been previously reported for estrone [43].

4. Discussion

Quinoid forming estrogens and SERMs have been associated with carcinogenesis [1, 44]. For example, it has been shown that estradiol is metabolized by cytochrome P450 to form 2- and 4-hydroxy catechols [44] which are further oxidized to *o*-quinones. 4-Hydroxyestradiol has been proposed to be more genotoxic, because the corresponding *o*-quinone can react with DNA to form DNA adducts or induce DNA oxidation leading to initiation and/or promotion of the carcinogenic process [44]. Similarly, the prototypical SERM tamoxifen has been shown to be metabolized to reactive quinoids by P450 isozymes, which could act as chemical carcinogens by modifying cellular macromolecules in addition to the carcinogenic carbocation pathway [16, 45–47]. Finally, Cavalieri has proposed *o*-quinone formation as a general genotoxic pathway for all aromatic compounds capable of forming *o*-quinones;

including benzene, naphthalene, catecholamines, as well as various endogenous and environmental estrogens [48].

While there have been studies on the formation and reactivity of quinoids formed from estrogens and SERMs [1, 44], a wider range of SERMs are required to provide more comprehensive structure-bioactivation correlations. LY2066948 is a novel SERM which is in development by Eli Lilly for the potential treatment of uterine fibroids and myomas [25]. In the current study, the superior antiestrogenic potency of LY2066948, as compared to 4-hydroxytamoxifen, was confirmed in cell cultures (Figure 1) [6, 25]. These data suggest that LY2066948 has promise as a potential new SERM. However, LY2066948 shares a naphthol scaffold similar to that of equilenin (Scheme 1) and is potentially susceptible to oxidative metabolism to electrophilic/redox active *o*-quinones in an analogous manner. For the case of equilenin, such *o*-quinones have previously been reported to mediate this estrogen's toxicity [44].

LY2066948 was synthesized as described previously with minor modification [25] and its oxidative chemistry examined using IBX to chemically generate *o*-quinone. IBX has been previously used to efficiently generate *o*-quinones from estrone, genestein [49–51], and in this study, from equilenin. Our data demonstrate that LY2066948-*o*-quinone is more stable ($t_{1/2} = 3.9$ h) than that of 4-OHEN-*o*-quinone ($t_{1/2} = 2.3$ h) (Figure 2). The presence of extra aryl substituents on LY2066948-*o*-quinone likely increases stability. Thompson et al. hypothesized that a “reactivity window” exists for quinone toxicity, with lifetimes in the 10 s – 10 min range resulting in cytotoxicity. More reactive quinones are argued to react immediately with solvent or the enzyme responsible for their formation [18, 52]. Similarly, Gross et al. proposed that long-lived quinones are more genotoxic [49] and supported this hypothesis with data for 4-OHE-*o*-quinone ($t_{1/2} = 12$ min) [53], which is more genotoxic than the *o*-quinones from 2-OHE ($t_{1/2} = 42$ s) [53] and genistein catechol ($t_{1/2} = 4$ s) [49]. According to these hypotheses, an LY2066948-*o*-quinone could potentially contribute to cytotoxicity or genotoxicity of LY2066948 through modification of cellular macromolecules, e.g. DNA, proteins, and lipids.

When LY2066948 or equilenin were incubated with GSH and tyrosinase, a dinuclear copper dependent monophenolmonooxygenase (EC 1.14.18.1) that has been shown to oxidize phenols to catechols and *o*-quinones [50, 54, 55], mono and di GSH conjugates were produced (Figure 3). Interestingly, when LY2066948 was incubated with tyrosinase in the presence of ascorbate, exclusive conversion of LY2066948 to the catechol occurred (Figure 3A). This method could also be used to synthesize catechols from equine estrogens. For example, when equilenin was incubated with tyrosinase in the presence of ascorbate a complete conversion of equilenin to 4-OHEN was observed (Figure 3B). According to Liehr's studies [23], hydroxylation at the 2-position of equilenin disrupts the aromaticity of the aromatic B-ring; therefore equilenin is converted exclusively to 4-OHEN by oxidative enzymes. It is reasonable to propose that the C-4 position on the A ring of LY2066948 is also the most active site for oxidation to generate corresponding catechol and *o*-quinone.

In rat liver microsomal incubations of LY2066948 in the presence of GSH and NADPH, one di-GSH *o*-quinone conjugate (Figure 5A) was detected as a minor metabolite. Similar microsomal experiments with equilenin generated considerably more *o*-quinone GSH conjugates as compared to LY2066948 (Figure 5B). Oxidative metabolism of LY2066948 by rat liver microsomes or CYP3A4 mainly occurred on the amino side chain to yield the *N*-dealkylated metabolite (Figure 5A). The piperidine moiety of LY2066948 appears to be a metabolic “soft spot” which directs the majority of oxidative metabolism away from the naphthol ring. Piperidine and related amino groups are common structural features in the side chains of benzothiophene and dihydrobenzoxathiin SERMs, and similar metabolic *N*-

dealkylation was observed with these two scaffolds to give primary amine metabolites [56, 57]. The electron-withdrawing methyl sulfonyl group of LY2066948 would be expected to decrease the oxidation potential of the naphthol ring, however the long half-life observed for LY2066948 *o*-quinone suggests that it is substrate orientation at the enzyme active site and the susceptibility of piperidine to oxidation that accounts for the experimental observations.

As mentioned earlier, CYP1B1 is one of the key enzymes responsible for oxidative metabolism of estrogens generating genotoxic *o*-quinones [24]. It is primarily expressed in the breast, ovary, and the uterus [58] which are the target tissues of LY2066948. In our studies, one mono and two di-GSH conjugates were detected when equilenin was incubated with CYP1B1 (Figure 6B), however LY2066948 does not appear to be a substrate of this isozyme since no GSH conjugates or any other oxidative metabolites were detected in these incubations (Figure 6A).

In conclusion, this study has shown that LY2066948 can be oxidized both chemically and enzymatically to a potentially cytotoxic, *o*-quinone, analogous to equilenin. However, in microsomal and CYP3A4 supersomal incubations with LY2066948 the presence of the piperidine side chain directs metabolism from primarily aromatic hydroxylation and 2-electron oxidation in the case of equilenin, to N-dealkylation for LY2066948. Therefore we do not believe that quinone formation from LY2066948 represents a major bioactivation pathway, nor is it likely to contribute substantially to *in vivo* toxicity for this SERM. This study highlights the importance of developing a complete understanding of the effect of structure alterations on the relative importance of the quinone cytotoxic pathway for SERMs, estrogens, and phenolic compounds in general.

Acknowledgments

This research was supported by NIH Grant CA79870. We thank Dr. V.C. Jordan for providing MCF-7 WS8 cells as well as pERE-luciferase plasmids. We would also like to thank Dr. R. B. Hochberg for providing Ishikawa/ECC-1 cells, and Dr. Birgit Dietz for performing cell line authentication experiments.

Abbreviations

DMA	desmethylarzoxifene
E₂	17 β -estradiol, 1,3,5(10)-estratrien-3,17 β -diol
EN	equilenin, 1,3,5(10),6,8-estropentaen-3-ol-17-one
ER	estrogen receptor
HRT	hormone-replacement therapy
HPLC	high-performance liquid chromatography
4-OHEN	4-hydroxyequilenin, 1,3,5(10),6,8,-estrapentaen-3,4-diol-17-one
4-OHEQ	4-hydroxyequilin, 1,3,5(10), 7-estratetraen-3,4-diol-17-one; 4-OHE, 4-hydroxyestrone, 1,3,5(10)-estratrien-3,4-diol-17-one
IBX	2-iodoxybenzoic acid
LC-MS/MS	liquid chromatography-tandem mass spectrometry
LY2066948	6-(4-methanesulfonylphenyl)-5-[4-(2-piperidin-1-ylethoxy)phenoxy]-naphthaten-2-ol
P450	cytochrome P450
SERM	selective estrogen receptor modulator

TYR tyrosinase**References**

1. Dowers TS, et al. Bioactivation of selective estrogen receptor modulators (SERMs). *Chem. Res. Toxicol.* 2006; 19(9):1125–37. [PubMed: 16978016]
2. Pickar JH, MacNeil T, Ohleth K. SERMs: progress and future perspectives. *Maturitas.* 2010; 67(2): 129–138. [PubMed: 20580502]
3. Shelly W, et al. Selective estrogen receptor modulators: an update on recent clinical findings. *Obstet. Gynecol. Surv.* 2008; 63(3):163–81. [PubMed: 18279543]
4. King CM. Tamoxifen and the induction of cancer. *Carcinogenesis.* 1995; 16(7):1449–54. [PubMed: 7614676]
5. Taylor HS. Designing the ideal selective estrogen receptor modulator--an achievable goal? *Menopause.* 2009; 16(3):609–615. [PubMed: 19182697]
6. Geiser AG, et al. A new selective estrogen receptor modulator with potent uterine antagonist activity, agonist activity in bone, and minimal ovarian stimulation. *Endocrinology.* 2005; 146(10): 4524–35. [PubMed: 16002528]
7. Palacios S. Efficacy and safety of bazedoxifene, a novel selective estrogen receptor modulator for the prevention and treatment of postmenopausal osteoporosis. *Curr. Med. Res. Opin.* 2010; 26(7): 1553–1563. [PubMed: 20429824]
8. Cummings SR, et al. Lasofoxifene in postmenopausal women with osteoporosis. *N. Engl. J. Med.* 2010; 362(8):686–696. [PubMed: 20181970]
9. Fisher B, et al. Tamoxifen for prevention of breast cancer: report of the National Surgical Adjuvant Breast and Bowel Project P-1 Study. *J. Natl. Cancer Inst.* 1998; 90(18):1371–88. [PubMed: 9747868]
10. Jordan VC, Morrow M. Tamoxifen, raloxifene, and the prevention of breast cancer. *Endocr. Rev.* 1999; 20(3):253–78. [PubMed: 10368771]
11. Pinkerton JV, Goldstein SR. Endometrial safety: a key hurdle for selective estrogen receptor modulators in development. *Menopause.* 2010; 17(3):642–653. [PubMed: 20107426]
12. Bolton JL. Quinoids, quinoid radicals, and phenoxyl radicals formed from estrogens and antiestrogens. *Toxicology.* 2002; 177(1):55–65. [PubMed: 12126795]
13. Bolton JL, et al. Role of quinones in toxicology. *Chem. Res. Toxicol.* 2000; 13(3):135–60. [PubMed: 10725110]
14. Beland FA, et al. Analysis of tamoxifen-DNA adducts in endometrial explants by MS and 32P-postlabeling. *Biochem. Biophys. Res. Commun.* 2004; 320(2):297–302. [PubMed: 15219826]
15. Jordan VC. Selective estrogen receptor modulation: concept and consequences in cancer. *Cancer Cell.* 2004; 5(3):207–13. [PubMed: 15050912]
16. Shibutani S, et al. Tamoxifen-DNA adducts detected in the endometrium of women treated with tamoxifen. *Chemical Research in Toxicology.* 1999; 12(7):646–53. [PubMed: 10409405]
17. Fan PW, Zhang F, Bolton JL. 4-Hydroxylated metabolites of the antiestrogens tamoxifen and toremifene are metabolized to unusually stable quinone methides. *Chem. Res. Toxicol.* 2000; 13(1):45–52. [PubMed: 10649966]
18. Liu J, et al. Bioactivation of the selective estrogen receptor modulator acolbifene to quinone methides. *Chem. Res. Toxicol.* 2005; 18(2):174–82. [PubMed: 15720121]
19. Yu L, et al. Oxidation of raloxifene to quinoids: potential toxic pathways via a diquinone methide and o-quinones. *Chemical Research in Toxicology.* 2004; 17(7):879–88. [PubMed: 15257612]
20. Liu H, et al. Bioactivation of the selective estrogen receptor modulator desmethylated arzoxifene to quinoids: 4'-fluoro substitution prevents quinoid formation. *Chem. Res. Toxicol.* 2005; 18(2):162–73. [PubMed: 15720120]
21. Chen Y, et al. The equine estrogen metabolite 4-hydroxyequilenin causes DNA single-strand breaks and oxidation of DNA bases in vitro. *Chem. Res. Toxicol.* 1998; 11(9):1105–11. [PubMed: 9760286]

22. Shen L, et al. Bioreductive activation of catechol estrogen-ortho-quinones: aromatization of the B ring in 4-hydroxyequilenin markedly alters quinoid formation and reactivity. *Carcinogenesis*. 1997; 18(5):1093–101. [PubMed: 9163701]
23. Sarabia SF, et al. Mechanism of cytochrome P450-catalyzed aromatic hydroxylation of estrogens. *Chem. Res. Toxicol.* 1997; 10(7):767–71. [PubMed: 9250410]
24. Spink DC, et al. Metabolism of equilenin in MCF-7 and MDA-MB-231 human breast cancer cells. *Chem. Res. Toxicol.* 2001; 14(5):572–81. [PubMed: 11368557]
25. Hummel CW, et al. A selective estrogen receptor modulator designed for the treatment of uterine leiomyoma with unique tissue specificity for uterus and ovaries in rats. *J. Med. Chem.* 2005; 48(22):6772–5. [PubMed: 16250633]
26. Chen Y, et al. A metabolite of equine estrogens, 4-hydroxyequilenin, induces DNA damage and apoptosis in breast cancer cell lines. *Chem. Res. Toxicol.* 2000; 13(5):342–50. [PubMed: 10813650]
27. Liu X, et al. Oxidative DNA Damage Induced by Equine Estrogen Metabolites: Role of Estrogen Receptor. *Chem. Res. Toxicol.* 2002; 15(4):512–519. [PubMed: 11952337]
28. Zhang F, et al. Equine estrogen metabolite 4-hydroxyequilenin induces DNA damage in the rat mammary tissues: formation of single-strand breaks, apurinic sites, stable adducts, and oxidized bases. *Chem. Res. Toxicol.* 2001; 14(12):1654–9. [PubMed: 11743748]
29. NIH. NIH Guidelines for the Laboratory Use of Chemical Carcinogens, U.G.P.O., 2381–2385. NIH; Washington, DC: 1981.
30. Marcoux J-F, Doye S, Buchwald SL. A General Copper-Catalyzed Synthesis of Diaryl Ethers. *Journal of the American Chemical Society*. 1997; 119(43):10539–10540.
31. Pink JJ, et al. An estrogen-independent MCF-7 breast cancer cell line which contains a novel 80-kilodalton estrogen receptor-related protein. *Cancer Research*. 1995; 55(12):2583–90. [PubMed: 7780972]
32. Pink JJ, Jordan VC. Models of estrogen receptor regulation by estrogens and antiestrogens in breast cancer cell lines. *Cancer Research*. 1996; 56(10):2321–30. [PubMed: 8625307]
33. Ariazi EA, et al. Estrogen induces apoptosis in estrogen deprivation-resistant breast cancer through stress responses as identified by global gene expression across time. *Proceedings of the National Academy of Sciences of the United States of America*. 2011; 108(47):18879–86. [PubMed: 22011582]
34. Littlefield BA, et al. A simple and sensitive microtiter plate estrogen bioassay based on stimulation of alkaline phosphatase in Ishikawa cells: estrogenic action of delta 5 adrenal steroids. *Endocrinology*. 1990; 127(6):2757–62. [PubMed: 2249627]
35. Pisha E, Pezzuto JM. Cell-based assay for the determination of estrogenic and anti-estrogenic activities. *Methods Cell Sci.* 1997; 19:37–43.
36. Holinka CF, et al. Effects of steroid hormones and antisteroids on alkaline phosphatase activity in human endometrial cancer cells (Ishikawa line). *Cancer Res.* 1986; 46(6):2771–4. [PubMed: 2938730]
37. Overk CR, et al. High-content screening and mechanism-based evaluation of estrogenic botanical extracts. *Comb. Chem. High Throughput Screen.* 2008; 11(4):283–93. [PubMed: 18473738]
38. Thompson JA, et al. Oxidative metabolism of butylated hydroxytoluene by hepatic and pulmonary microsomes from rats and mice. *Drug Metab. Dispos.* 1987; 15(6):833–40. [PubMed: 2893710]
39. Horwitz KB, Costlow ME, McGuire WL. MCF-7; a human breast cancer cell line with estrogen, androgen, progesterone, and glucocorticoid receptors. *Steroids*. 1975; 26(6):785–795. [PubMed: 175527]
40. Dieckhaus CM, et al. Negative ion tandem mass spectrometry for the detection of glutathione conjugates. *Chem. Res. Toxicol.* 2005; 18(4):630–8. [PubMed: 15833023]
41. Chang M, et al. Inhibition of glutathione S-transferase activity by the quinoid metabolites of equine estrogens. *Chem. Res. Toxicol.* 1998; 11(7):758–65. [PubMed: 9671538]
42. Guengerich FP. Cytochrome P-450 3A4: regulation and role in drug metabolism. *Annu. Rev. Pharmacol. Toxicol.* 1999; 39:1–17. [PubMed: 10331074]

43. Lee AJ, et al. Characterization of the oxidative metabolites of 17beta-estradiol and estrone formed by 15 selectively expressed human cytochrome p450 isoforms. *Endocrinology*. 2003; 144(8): 3382–98. [PubMed: 12865317]
44. Bolton JL, Thatcher GR. Potential mechanisms of estrogen quinone carcinogenesis. *Chem. Res. Toxicol.* 2008; 21(1):93–101. [PubMed: 18052105]
45. Beland FA, et al. Tamoxifen-DNA adduct formation in human endometrium. *Chem. Res. Toxicol.* 2005; 18(10):1507–9. author reply 1509–11. [PubMed: 16533012]
46. Fan PW, Bolton JL. Bioactivation of tamoxifen to metabolite E quinone methide: reaction with glutathione and DNA. *Drug Metab. Dispos.* 2001; 29(6):891–6. [PubMed: 11353759]
47. Shibutani S, et al. Identification of tamoxifen-DNA adducts in the endometrium of women treated with tamoxifen. *Carcinogenesis*. 2000; 21(8):1461–7. [PubMed: 10910945]
48. Cavalieri EL, Rogan EG. Is bisphenol A a weak carcinogen like the natural estrogens and diethylstilbestrol? *IUBMB Life*. 2010; 62(10):746–51. [PubMed: 20945454]
49. Zhang Q, et al. Balance of beneficial and deleterious health effects of quinones: a case study of the chemical properties of genistein and estrone quinones. *J. Am. Chem. Soc.* 2009; 131(3):1067–76. [PubMed: 19115854]
50. Pezzella A, et al. Tyrosinase-catalyzed oxidation of 17beta-estradiol: structure elucidation of the products formed beyond catechol estrogen quinones. *Chem. Res. Toxicol.* 2005; 18(9):1413–9. [PubMed: 16167833]
51. Magdziak D, et al. Regioselective oxidation of phenols to o-quinones with o-iodoxybenzoic acid (IBX). *Org. Lett.* 2002; 4(2):285–8. [PubMed: 11796071]
52. Thompson DC, et al. o-Methoxy-4-alkylphenols that form quinone methides of intermediate reactivity are the most toxic in rat liver slices. *Chemical Research in Toxicology*. 1995; 8(3):323–7. [PubMed: 7578916]
53. Iverson SL, et al. Bioactivation of Estrone and Its Catechol Metabolites to Quinoid-Glutathione Conjugates in Rat Liver Microsomes. *Chem. Res. Toxicol.* 1996; 9(2):492–499. [PubMed: 8839054]
54. Moridani MY, et al. Catechin metabolism: glutathione conjugate formation catalyzed by tyrosinase, peroxidase, and cytochrome P450. *Chem. Res. Toxicol.* 2001; 14(7):841–8. [PubMed: 11453730]
55. Sanchez-Ferrer A, et al. Tyrosinase: a comprehensive review of its mechanism. *Biochim. Biophys. Acta*. 1995; 1247(1):1–11. [PubMed: 7873577]
56. Qin Z, et al. Structural modulation of oxidative metabolism in design of improved benzothiophene selective estrogen receptor modulators. *Drug Metab. Dispos.* 2009; 37(1):161–9. [PubMed: 18936111]
57. Zhang Z, et al. In vitro bioactivation of dihydrobenzoxathiin selective estrogen receptor modulators by cytochrome P450 3A4 in human liver microsomes: formation of reactive iminium and quinone type metabolites. *Chem. Res. Toxicol.* 2005; 18(4):675–85. [PubMed: 15833027]
58. Yager JD, Davidson NE. Estrogen carcinogenesis in breast cancer. *N. Engl. J. Med.* 2006; 354(3): 270–82. [PubMed: 16421368]

Highlights

- SERM LY2066948, similar to the estrogen equilenin (EN), is oxidized to a catechol.
- Incubations of LY2066948 and EN with oxidative enzyme and GSH gave GSH conjugates.
- Side chain *N*-dealkylation is the major metabolic pathway of LY2066948 by P450s.
- Structural alterations determine quinone formation and potential cytotoxicity.

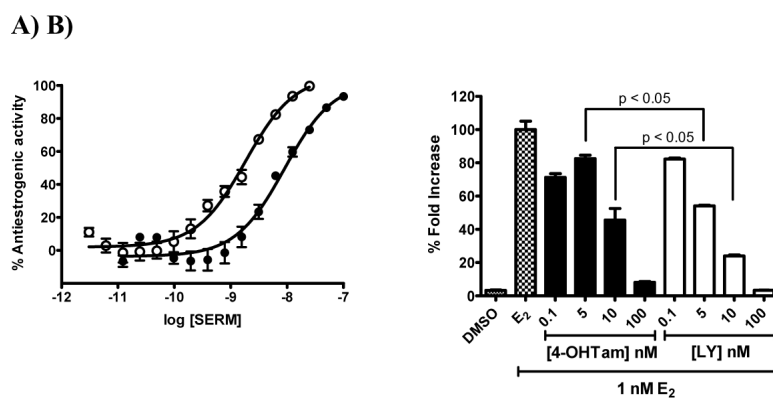


Figure 1.

(A) Ishikawa Alkaline Phosphatase Assay: Relative activity of alkaline phosphatase after treatment of Ishikawa cells (5×10^4 cells/well) with different concentrations of LY2066948 (opened circles) and 4-OH tamoxifen (closed circles) in the presence of 0.9 nM E_2 for 72 h. LY2066948, $IC_{50} = 1.8 \pm 0.50$ nM; 4-hydroxytamoxifen, $IC_{50} = 9.0 \pm 1.9$ nM. Experimental details are described in the Material and Methods. (B) Induction of ERE-luciferase reporter activity in MCF-7 WS-8 cells. Cells were transiently transfected with ERE-luciferase reporter gene and pRL-TK. The transfected cells were treated with various concentrations of LY2066948 and 4-OH tamoxifen in the presence of 1 nM E_2 for 24 h.

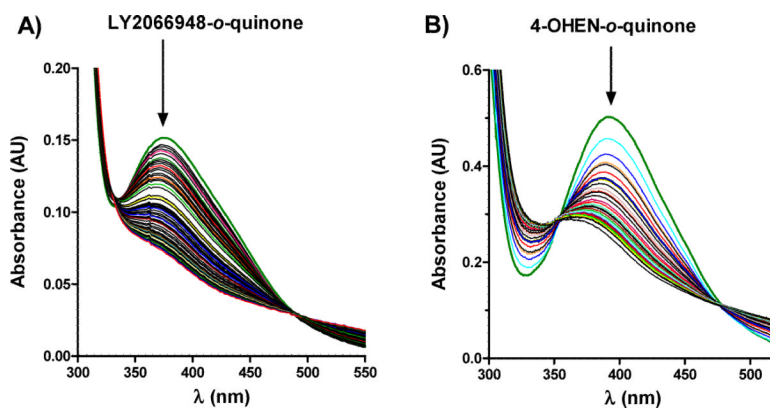


Figure 2. The decomposition of (A) LY2066948-*o*-quinone (60 μ M) and (B) 4-OHEN-*o*-quinone (60 μ M) in 50 mM phosphate buffer (pH 7.4, 37 $^{\circ}$ C) were monitored at 378 and 392 nm, respectively. Representative UV spectra were recorded continuously from 300 to 600 nm at 10 min/scan. Approximate half-lives were found to be 3.9 ± 0.1 h and 2.5 ± 0.2 h, respectively.

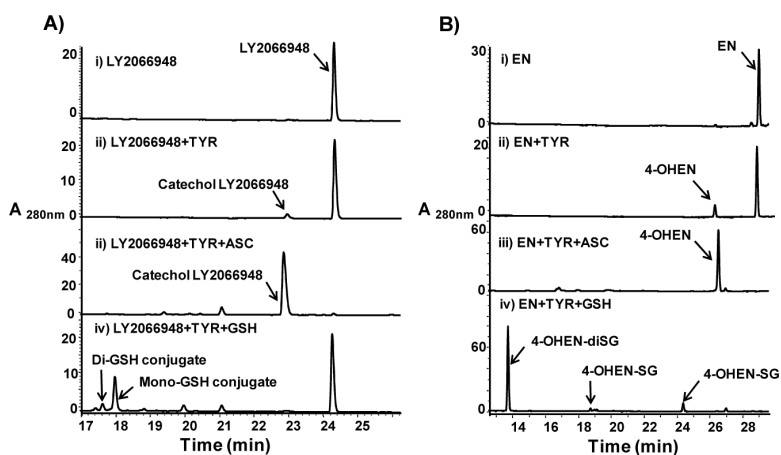


Figure 3. Oxidation of LY2066948 and EN by tyrosinase. HPLC chromatograms of incubations of (A) LY2066948 (30 μ M) and (B) EN (30 μ M) with 0.1 mg/mL of tyrosinase (TYR), 1 mM of ascorbic acid (ASC), and 1 mM of GSH in 50 mM phosphate buffer (pH 7.4, 0.5 mL total volume) for 30 min at 37 $^{\circ}$ C. Metabolites and GSH conjugates were detected by UV-visible absorbance (shown in arbitrary units) at 280 nm and all annotated peaks were characterized by LC-MS/MS.

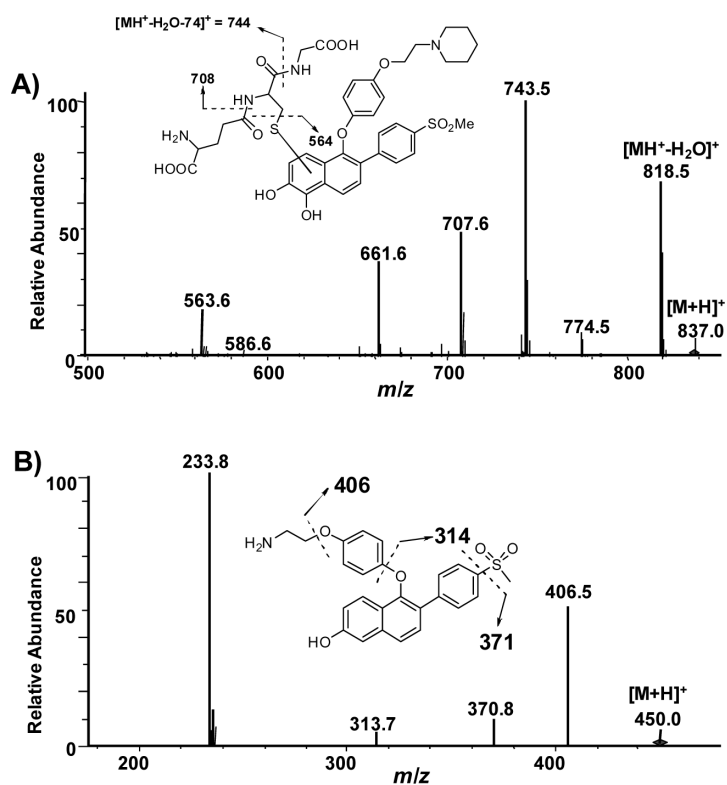


Figure 4. Mass spectrometric analysis of LY2066948 metabolites. (A) MS/MS spectrum of the LY2066948 mono-GSH conjugate. (B) MS/MS spectrum of *N*-dealkylated metabolite of LY2066948.

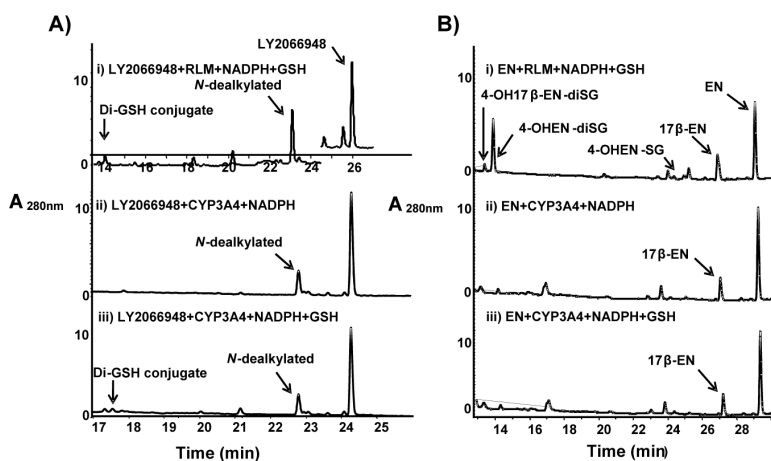


Figure 5.

Representative chromatograms of incubations of (A) LY2066948 (30 μM) and (B) EN (30 μM) with either rat liver microsomes (RLM) (1 nmol of P450/mL) or CYP3A4 (10 pmol/mL), NADPH (1 mM), and GSH (1 mM) in 50 mM phosphate buffer (pH 7.4, 0.5 mL total volume) for 30 min at 37 °C. Metabolites and GSH conjugates were detected by UV-visible absorbance (shown in arbitrary units) at 280 nm, and all annotated peaks were characterized by LC-MS/MS analysis. Metabolites and GSH conjugates for RLM incubations of LY2066948 were detected using HPLC method B.

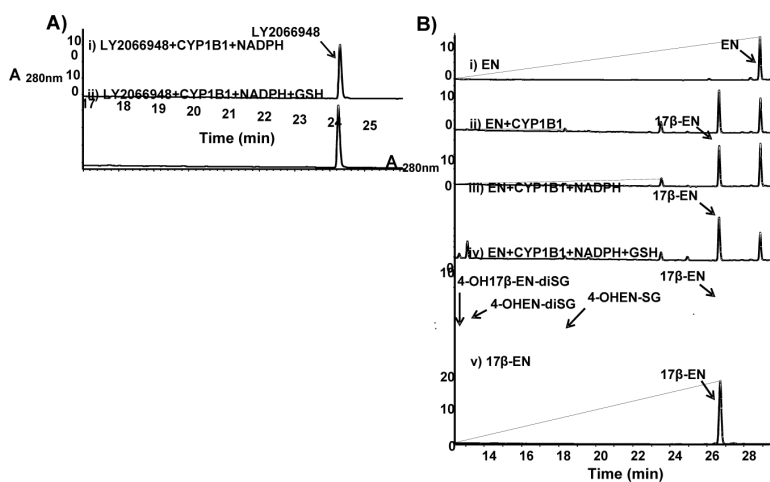
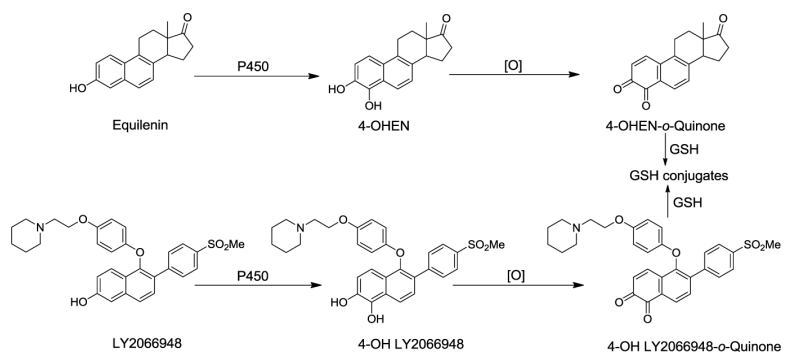
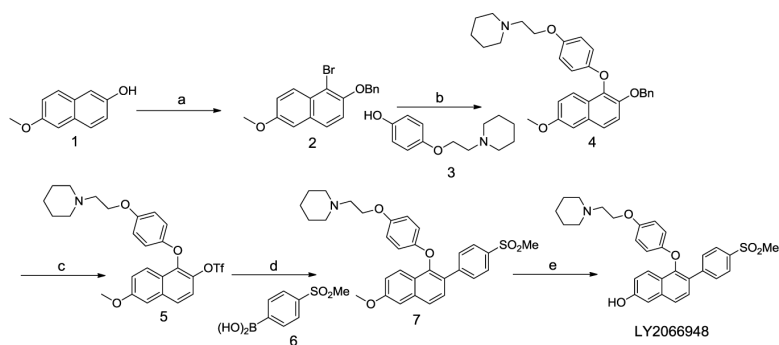


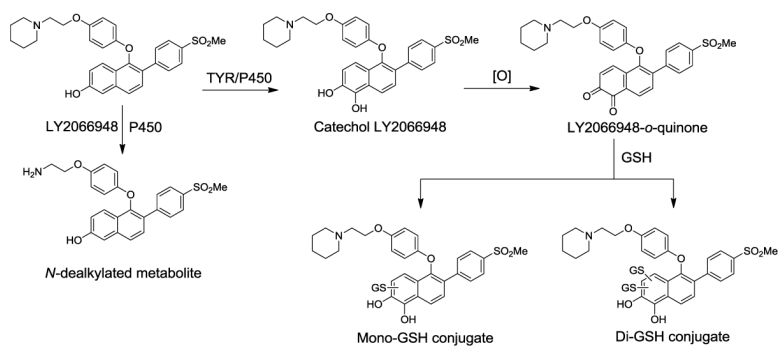
Figure 6. Representative chromatograms of incubations of (A) LY2066948 (30 μM) and (B) EN (30 μM) with CYP1B1 (10 pmol/mL), NADPH (1 mM), and GSH (1 mM) in 50 mM phosphate buffer (pH 7.4, 0.5 mL total volume) for 30 min at 37 °C. Metabolites and conjugates were detected by UV-visible absorbance (shown in arbitrary units) at 280 nm and all annotated peaks were characterized by LC-MS/MS analysis.



Scheme 1.
Proposed bioactivation of LY2066948 compared to equilenin.

**Scheme 2.**

Synthesis of LY2066948 (a) (i) NBS; (ii) BnBr; (b) Cu(OTf)₂, Cs₂CO₃, 1-naphtholic acid, **3**; (c) (i) Pd(OH)₂; (ii) Tf₂O; (d) Pd(OAc)₂, PCy₃, 4-(methanesulphonyl) phenylboronic acid (e) BBr₃.



Scheme 3.
Proposed metabolic pathways of LY2066948.